Available online at www.sciencedirect.com
SCIENCE DIRECT®
Applied Catalysis B: Environmental 49 (2004) 187–193
APPLIED CATALYSIS B: ENVIRONMENTAL
www.elsevier.com/locate/apcatb

Inhibition effect of SO_2 on NO_x and VOCs during the photodegradation of synchronous indoor air pollutants at parts per billion (ppb) level by TiO_2

C.H. Ao [a], S.C. Lee [a,*], S.C. Zou [b], C.L. Mak [c]

[a] *Department of Civil & Structural Engineering, Research Center for Urban Environmental Technology and Management, The Hong Kong Polytechnic University, Hong Kong, China*
[b] *School of Chemistry and Chemical Engineering, Zhongshan University, Guangzhou, China*
[c] *Department of Applied Physics, The Hong Kong Polytechnic University, Hong Kong, China*

Received 9 October 2003; received in revised form 1 December 2003; accepted 8 December 2003

Abstract

Sulfur-containing compounds are well-known catalyst poisons. To evaluate the feasibility of photocatalytic technology for indoor air purification, a typical atmospheric SO_2 concentration of 200 parts per billion (ppb) was selected. In order to further evaluate the impact of SO_2 on the photocatalytic activity of other typical indoor air pollutants, SO_2 was co-injected with 200 ppb NO and 20 ppb benzene, toluene, ethylbenzene, and *o*-xylene (BTEX) using TiO_2 (P-25) as photocatalyst coated on a glass fiber filter. A concurrent photodegradation of SO_2 with NO, SO_2 with BTEX, and SO_2 with NO and BTEX was also conducted. Results showed that no photodegradation of SO_2 was found. However, the blank glass fiber filter adsorbed more than 75% of the SO_2. The conversion of NO decreased by 8% and the generation of NO_2 increased by 10% with the presence of SO_2. A similar inhibition effect was found on the photodegradation of BTEX with the presence of SO_2. The presence of SO_2 decreased the conversion of BTEX by more than 10%. Ion chromatography analysis on the TiO_2 glass fiber filter showed that sulfate ion was formed from the adsorption of SO_2. The formation of sulfate ion inhibited the formation of nitrate ion, which increased the generation of NO_2. It is suggested that the inhibition effect of SO_2 is due to the sulfate ion competing with the pollutant for adsorption sites on TiO_2. The promotion effect of NO on BTEX was also reduced by the presence of SO_2.

Keywords: Titanium dioxide; BTEX; Photocatalyst; Trace level

1. Introduction

Numerous studies [1–5] have shown that the quality of indoor air has a direct impact on human health. Thus the improvement of indoor air quality is of importance. Traditionally, air pollutants are mainly removed by adsorption. However, adsorption only transfers pollutants from the gaseous phase to the solid phase and eventually causes disposal problems.

Photocatalysis provides a very promising solution for pollutant removal as the pollutants are actually oxidized and converted to compounds such as CO_2 and H_2O [6–9]. However, only a few studies have been reported on the photodegradation of multiple air pollutants. The inhibition and promotion effects in the photodegradation of the mixtures of methylene chloride, methanol, carbon tetrachloride and 2-propanol were reported [10]. Ollis and coworkers [11–13] have conducted a comprehensive study on the binary photodegradation of chlorinated hydrocarbon and organic compounds. Trichloroethylene was found to promote the conversion of toluene. The above studies, however, used a pollutant concentration at several hundreds ppm level which is not found in normal and heavily polluted indoor air. The photodegradation of multiple air pollutants, especially those at typical indoor air ppb level, is rare. Previously, we reported the photoreaction between NO and BTEX [14], NO, NO_2, and CO [15] using typical indoor ppb level concentrations. Although it is not possible to evaluate the interactions of all indoor air pollutants by photocatalysis, a study of the interactions between the major and common pollutants using photocatalysis is feasible and valuable.

* Corresponding author. Tel.: +852-2766-6011; fax: +852-2334-6389.
E-mail address: ceslee@polyu.edu.hk (S.C. Lee).

0926-3373/$ – see front matter © 2003 Elsevier B.V. All rights reserved.
doi:10.1016/j.apcatb.2003.12.011

Sulfur dioxide (SO_2) is selected as the target pollutant because it has an adverse impact on human health [16,17]. Study [18] showed that respiratory and cardiovascular deaths were reduced with decreasing SO_2 concentration. The annual average SO_2 concentration [19] can reach as high as 180 ppb. Previous study showed that both homogeneous and heterogeneous reaction occurred on SO_2. When heptane was co-injected with SO_2, the photodegradation rate of SO_2 decreased. Deactivation was also reported for SO_2 [20]. However, the concentration of SO_2 in the above study is 4000 ppm, which is almost 20 000 times that of indoor SO_2 levels. In this study, 200 ppb of SO_2 is selected with reference to the SO_2 concentration in China. This concentration is also selected in order to compare the effect of NO on BTEX used in our previous studies. Two hundred parts per billion NO [21,22] is selected with reference to the typical indoor air pollutant level. Twenty parts per billion benzene, toluene, ethylbenzene, and *o*-xylene (BTEX) are selected, as BTEX is the most commonly found VOCs in indoor environment [3,23,24]. The aim of this study is to evaluate the photodegradation of SO_2 under typical indoor environmental conditions. The effects of residence time and levels of humidity on the photodegradation rate are also conducted, as these are the vital parameters for photocatalytic indoor air purification [14,15]. As a sulfur-containing compound is usually poisonous to the catalyst [25–27], investigating the photodegradation of NO and BTEX with the presence of SO_2 is valuable. In addition, the effect of the presence of SO_2 on the promotion effect of NO on BTEX is also investigated. To the best of our knowledge, no study has been reported for the concurrent photodegradation of NO, SO_2, and BTEX at trace level (ppb) concentrations.

2. Experimental

2.1. Reagents and catalyst

The detailed experimental setup has been described elsewhere [28]. BTEX (Spectra gases) with a mixing ratio of 1:1:1:1, NO (BOC gases) and SO_2 (BOC gases) were used as the reactant gas and acquired from a compressed gas cylinder at concentrations of 1 ppm ± 2%, 10 ppm ± 5%, and 50 ppm ± 2%, respectively, with nitrogen as balanced gas with traceable National Institute of Standards and Technology (NIST) standard. TiO_2 (Degussa P-25) was used as a photocatalyst. The catalyst was used as received without any pretreatment. Water suspensions of 5% TiO_2 were coated on a glass fiber filter (Whatman) over an area of 20 cm × 21 cm, as a supporting substrate (denoted as TiO_2 filter). It was then calcinated at 120 °C for 1 h with a temperature gradient of 5.5 °C/min. The amount of TiO_2 imposed is determined by the weight difference before and after the coating procedure. In all experiments, the weight of TiO_2 imposed is 1.64 g ± 5%.

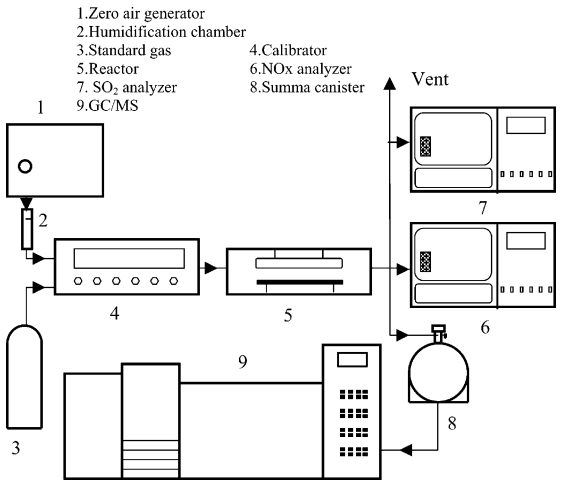

Fig. 1. Schematic diagram of the experimental setup.

2.2. Reactor and experimental setup

Fig. 1 shows a schematic diagram of the experimental setup for this study. A reactor with a volume of 18.6 l (20.1 cm × 44.2 cm × 21 cm) with its surface coated by a Teflon film (BYTAC Type AF-21) was used for this study. Illumination was provided by a 6 W UV lamp (Cole-Parmler) which emits a primary wavelength at 365 nm and its intensity was determined by a UV-meter (Spectroline DRC-100X). The UV lamp was horizontally placed at the upper part of the reactor, 14 cm from both ends. UV intensity measured in all experiments was 750 μW/cm^2. The TiO_2-coated filter was supported by a Teflon film and fixed horizontally with a vertical distance of 5 cm between the UV lamp. Stainless steel sampling ports and Teflon tubing were used to connect the reactor and the analytical instruments.

A zero air generator (Model 111, Thermo Environmental Instruments Inc.) was used to supply the air stream. The desired humidity of the flow was controlled by passing the zero air stream through a humidification chamber. The reactant stream and the zero air stream were connected to a mass flow calibrator (Model 700, Advanced Pollution Instrumentation Inc.). The gas streams were pre-mixed by a gas blender and the desired flow was controlled by a mass flow controller inside the calibrator. After the inlet and the outlet concentrations achieved equilibrium (1 h), the UV lamp was turned ON and initiated the reaction. The concentration of NO was continuously measured with a Chemiluminescence NO analyzer (Model 42c, Thermo Environmental Instruments Inc.), which monitors NO, NO_2, and NO_x at a sampling rate of 0.7 l/min. SO_2 was continuously measured with a Pulsed Fluorescence SO_2 analyzer (Model 43b, Thermo Environmental Instruments Inc.) at a sampling rate of 0.4 l/min. Pre-cleaned Summa canisters were evacuated for VOCs sampling. Constant VOCs sampling time was achieved using a mass flow controller. Samples of VOCs were collected at designated times during the experiment. After collection, the canister sample was first

concentrated by a Nutech Cryogenic Concentrator (Model 3550A), and the trapped VOCs were separated and analyzed by Hewlett-Packard Gas Chromatograph (Model HP 6890) and quantified by a Mass Selective Detector (Model HP5973). After analysis, the canister was sequentially evacuated and pressurized with humidified zero air until all compounds detected were smaller than 0.2 ppb. TO-14 (Toxi-Mat-14M Certified Standard (Matheson)) standard gas was analyzed using the GC–MS system seven times at 0.2 ppb to obtain the method detection limits [3].

The concentration of the anion was conducted by immersing the TiO_2 filter into distilled deionized water for 24 h. The solution was then filtered through a 0.45 μm filter to avoid clogging the column. A Dionex ion chromatograph consisted of a gradient pump with an automatic membrane eluent degassing and a conductivity detector. The separations were performed on an IonPac AS14 anion-exchange column (150 mm × 4 mm i.d.) with an IonPac GS 14 Guard column (50 mm × 4 mm i.d.) at a rate of 1.2 ml/min (3.5 mmol/l Na_2CO_3 + 1.0 mmol/l $NaHCO_3$). All instrumental control, data collection, and processing were performed with the Netpeak chromatography station. The pH of the solution was measured with an Orion Expandable Ion Analyzer (EA 940) with a Cole-Parmer pH electrode.

3. Results and discussion

3.1. Photodegradation of SO_2

Prior to the photodegradation of SO_2, a photolysis test was conducted. No change in SO_2 concentration was observed passing through the reactor when only UV irradiation was presented. Table 1 shows the photodegradation of SO_2 at a humidity level of 2100 ppmv and at a residence time of 3.73 min both with and without the presence of UV irradiation. Around 75% of the SO_2 was adsorbed on the blank glass fiber filter. When the filter was imposed with TiO_2, the amount of SO_2 adsorbed between the blank filter and the TiO_2 filter is insignificant. Upon UV irradiation, the concentration of SO_2 was similar to the amount adsorbed on the blank filter. Thus, no photodegradation was found on the TiO_2 filter.

To further evaluate the photodegradation of SO_2, the same amount of TiO_2 powder was imposed on a Teflon plate having the same surface area of the glass fiber filter. Results showed that no adsorption in the dark or photodegradation of SO_2 under UV irradiation was found within the limit of the experimental error. This showed that SO_2 is primarily adsorbed on the glass fiber filter but not on TiO_2. No photodegradation of SO_2 was observed despite the kind of substrate used. The results of this study are different from those reported by Shang et al. [20]. The latter reported that both homogeneous and heterogeneous photooxidation reactions were observed when using a 400 W high-pressure mercury lamp and 4000 ppm SO_2. This discrepancy is probably due to the differences arising from the application of SO_2 concentration and the UV lamp. In this study, a 6 W UV lamp was used and the energy provided is probably not large enough to initiate the homogeneous reaction [29]. No heterogeneous photodegradation was observed in this study; this is probably due to the SO_2 concentration conducted is too low to be adsorbed on TiO_2. The photodegradation of CO [30] only occurred at a concentration higher than 140 ppm. No photodegradation was found for lower CO concentration owing to the low CO adsorbed on the photocatalyst active sites. Since the concentration conducted in this study is only 200 ppb, whereas 4000 ppm was used by Shang et al. [20], no photocatalytic heterogeneous reaction is due to the low adsorption of SO_2 on TiO_2 because only ppb levels of SO_2 were conducted in this study.

3.2. The impact on the photodegradation of NO with the presence of SO_2

Fig. 2(a) shows the photodegradation of NO with and without the presence of SO_2 under different humidity levels at a residence time of 1.24 min. The initial concentrations of NO and SO_2 were 200 ppb. The presence of SO_2 inhibited the conversion of NO despite the levels of humidity. The photodegradation of NO is adversely affected by increasing humidity levels [14,15]. Fig. 2(b) shows the generation of NO_2 from the photodegradation of NO. The experimental conditions are identical to that in Fig. 2(a). The presence of SO_2 not only inhibited the conversion of NO but also

Table 1
Photodegradation of SO_2 under different experimental conditions

Experimental conditions	Initial SO_2 concentration (ppb)	SO_2 concentration (ppb) at 120 min
UV lamp OFF		
TiO_2 powder (P-25)	200	198
Blank filter	200	51
TiO_2 filter (P-25)	200	46
UV lamp ON		
TiO_2 powder (P-25)	200	199
Blank filter	200	52
TiO_2 filter (P-25)	200	44

Humidity level: 2100 ppmv; residence time: 3.7 min.

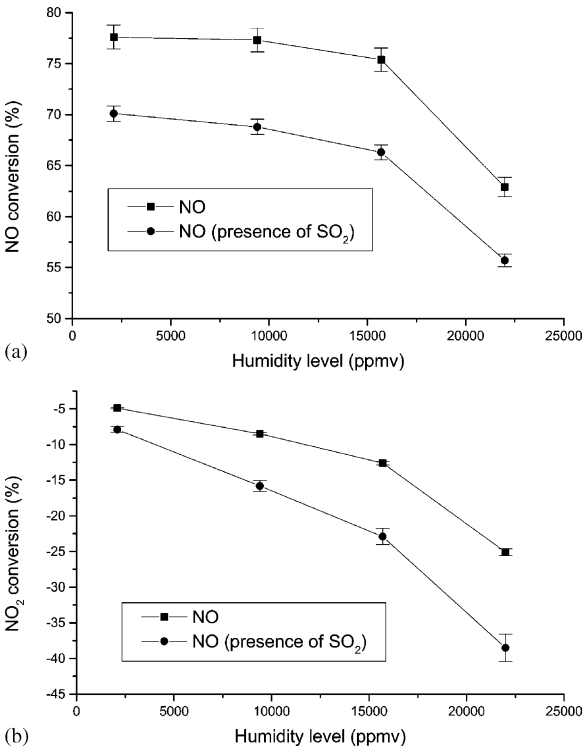

Fig. 2. (a) Conversion of NO with and without the presence of SO_2 at an initial concentration of 200 ppb NO and SO_2. Experimental conditions—residence time: 1.2 min; humidity level: 2100 ppmv. (b) Conversion of NO_2 with and without the presence of SO_2 at an initial concentration of 200 ppb NO and SO_2. Experimental conditions—residence time: 1.2 min; humidity level: 2100 ppmv.

increased the generation of NO_2. With the presence of SO_2, the NO_2 generation increased by 10%.

The binary photodegradation results of NO and CO [15] showed that no photodegradation of CO was found under different residence time and levels of humidity. The existence of CO does not promote or inhibit the photodegradation of NO. Although no photodegradation of SO_2 was found in this study, the existence of SO_2 reduced the conversion of NO and increased the generation of NO_2. The difference between the effects of SO_2 and CO is probably due to the product formed on the filter.

Fig. 3 shows the concentration of the sulfate ion (SO_4^{2-}) on the TiO_2 filter during the photodegradation of 200 ppb SO_2 at a residence time of 1.24 min at different humidity levels. The blank SO_4^{2-} concentration of the filter is 39 μg per filter and is subtracted from the SO_4^{2-} concentration presented in Fig. 3. The formation of SO_4^{2-} increased with increasing humidity levels. When the humidity level increased from 2100 to 22 000 ppmv, the amount of SO_4^{2-} also increased from 433 to 1395 μg per filter. SO_2 generated from the inlet stream was oxidized as SO_4^{2-} species and was deposited on the filter. As shown in the same figure, the pH value of the TiO_2 filter decreased from 10.02 to 9.61 when the humidity increased from 2100 to 22 000 ppmv. The results showed that the acidity on the TiO_2 glass fiber filter

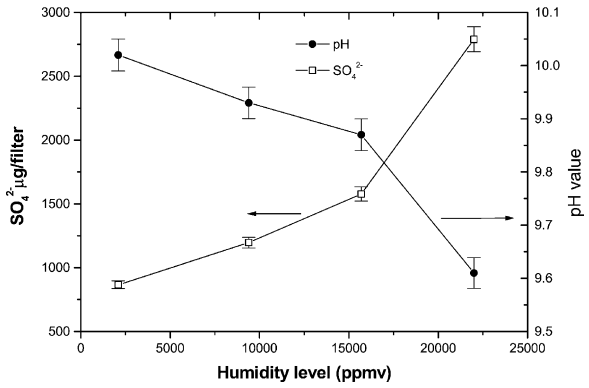

Fig. 3. Sulfate ion (SO_4^{2-}) concentration under different relative humidity levels at an initial concentration of 200 ppb SO_2. Experimental condition—residence: 1.2 min.

increased with increasing humidity levels. This is probably due to the adsorption of SO_2 on the filter that is converted into sulfuric acid. Sulfur dioxide is a highly soluble gas and absorbs water on the TiO_2 filter. It is then dissociated into hydrogen ion (H^+) and bisulfite (HSO_3^-) ion. The bisulfite is then further dissociated into sulfite ion (SO_3^{2-}) and reacted with oxygen forming sulfate ion (SO_4^{2-}), as shown in Eqs. (1)–(4) [31]:

$$SO_2 + H_2O \Leftrightarrow SO_2 \cdot H_2O \quad (1)$$

$$SO_2 \cdot H_2O \Leftrightarrow H^+ + HSO_3^- \quad (2)$$

$$HSO_3^- \Leftrightarrow H^+ + SO_3^{2-} \quad (3)$$

$$2SO_3^{2-} + O_2 \rightarrow 2SO_4^{2-} \quad (4)$$

Reactions (1)–(4) proceed without the presence of catalyst, though it is reported that the presence of iron catalyst increased the rate of reaction [32].

Another possible pathway of SO_4^{2-} ion formation is the reactions between SO_2 and HO_2 radicals, as shown in Eqs. (5)–(8) [29,33].

$$SO_2 + HO_2^\bullet \rightarrow SO_3 + OH^\bullet \quad (5)$$

$$SO_3 + H_2O \rightarrow H_2SO_4 \quad (6)$$

$$H_2SO_4 \rightarrow H^+ + HSO_4^- \quad (7)$$

$$HSO_4^- \rightarrow H^+ + SO_4^{2-} \quad (8)$$

Reactions (5)–(8) are likely not the sulfate ion formation pathway as sulfate ion was found even without the presence of UV light and TiO_2. The formation of sulfate ion from reactions (1)–(4) in this study is similar to the formation of acid rain. Studies [34–36] identified that the emission of SO_2 is a major cause of acid rain. SO_2 contacted with aerosols in the air. The wet surface of the aerosol provided a hydrated area for SO_2 to become into solution [37]. In this study, the glass fiber filter provided a surface area for the adsorption of SO_2. Zero air passing through the humidifier provided water vapor to the inlet stream. Oxygen supplied from zero

Table 2
Sulfate ion (SO_4^{2-}) and nitrate ion (NO_3^-) from the photodegradation of SO_2 and NO

Experimental conditions	SO_4^{2-} ions (μg per sheet)	NO_3^- ions (μg per sheet)
NO only	39	404
SO_2 only	417	49
NO and SO_2	448	162

Humidity level: 2100 ppmv; residence time: 1.2 min.

air reacted with sulfite ion forming sulfate ion on the filter. When TiO_2 powder was used without glass fiber filter as the supporting substrate, only a few ppb SO_2 differences were observed between the inlet stream and the outlet stream. Using a blank glass fiber filter only, similar SO_2 removal was observed compared to that of the TiO_2 filter. The IC result and the SO_2 concentration differences between the outlet stream and the inlet stream both supported the postulation that the adsorption of SO_2 had become SO_4^{2-}. In addition, the sulfate ion, SO_4^{2-}, is a frequently used indicator for the identification of acid rain [38,39] caused by the emission of SO_2.

The increase in NO_2 content is probably due to the presence of sulfate ion. NO is photodegraded to NO_2 and then converted to HNO_3 as is illustrated by the following equations [40,41]:

$$NO + HO_2^\bullet \rightarrow NO_2 + OH^\bullet \quad (9)$$

$$NO_2 + OH^\bullet \rightarrow HNO_3 \quad (10)$$

The nitric acid formed on the TiO_2 decreased the photoactivity and thus deactivation occurred [14,15,42]. Nitrate ion was used to identify the formation of nitric acid on TiO_2 [43]. According to Eqs. (9) and (10), NO_2 concentration is controlled by NO conversion rate. The presence of SO_2 inhibited the photodegradation of NO, and thus a lower NO_2 concentration is anticipated. The NO_2 concentration, however, increased despite a lower NO conversion. This is probably due to the generation of sulfate ion present before the start of the UV irradiation. The formation of HNO_3 from NO_2 at the initial stage of the NO photodegradation is inhibited. The sulfate ion blocked the adsorption sites of TiO_2 for converting NO_2 to HNO_3, leading to the increase of NO_2 exited to the outlet stream. The presence of SO_2 showed a clear inhibition effect not only on the target pollutant NO but also on the intermediate NO_2. The overall NO_x conversion decreased with the presence of SO_2.

Table 2 shows the concentrations of the sulfate ion and the nitrate ion from the photodegradation of NO, SO_2, and NO with SO_2. Sulfate ion and nitrate ion presented even though only NO and SO_2 was generated, respectively. This is due to the blank concentration of the sulfate and nitrate ion presented on the TiO_2 filter. When 200 ppb of NO is photodegraded, 404 μg per filter of nitrate ion was found. The nitrate ion was generated from the photodegradation of NO according to Eqs. (9) and (10). However, when SO_2 was co-injected with NO, the formation of nitrate ion decreased which is an indication of a decrease in HNO_3 formation. The presence of sulfate ion competed with nitrate ion for adsorption sites on TiO_2. Thus, the generation of NO_2 increased in the outlet stream. Study also showed that the presence of SO_4^{2-} ion decreased the photodecomposition of Astrazone Orange. The presence of adsorbed ion competed with the Astrazone Orange for adsorption sites on the TiO_2 surface [44]. The results of the sulfate ion and nitrate ion from IC analysis in this study indicated that the inhibition effect of SO_2 on the NO_x photodegradation is due to the presence of SO_4^{2-} ion. In the results shown in Table 1, we showed that no photodegradation of SO_2 occurred. Hence, the inhibition effect of SO_4^{2-} ion is due to the competition of adsorption sites between NO on the TiO_2 surface but not due to the competition of photoactive spices such as hydroxyl radicals.

3.3. Contemporaneous photodegradation of SO_2, NO, and BTEX

Fig. 4(a)–(d) shows the impact on the conversions of benzene, toluene, ethylbenzene, and *o*-xylene with the presence of SO_2, NO, and SO_2 with NO under a humidity level of 2100 ppmv and at a residence time of 1.24 min. Prior to the experiment, a blank test was conducted. No conversion of BTEX was observed with the presence of the TiO_2 filter and with the absence of UV irradiation. Conversion was also not observed with the presence of UV irradiation and the absence of a TiO_2 filter [14,15]. As shown in these figures, the presence of NO, SO_2, or NO with SO_2 showed a similar photodegradation profile with respect to the irradiation time and all cases reached a photosteady-state concentration at an irradiation time of 120 min.

The inhibition effect of SO_2 was observed in the conversions of BTEX. The presence of SO_2 reduced the conversions of benzene, toluene, ethylbenzene, and *o*-xylene by 18, 15.6, 6.4 and 3.9%, respectively, compared to the photodegradation of BTEX only. The inhibition effect of SO_2, however, is not the same as for BTEX. The addition of SO_2 resulted in the largest inhibition effects for benzene and the smallest for *o*-xylene. This is probably due to the reaction rate of *o*-xylene, with hydroxyl radicals being comparatively higher than benzene [45]. The inhibition effect of SO_2 may be hindered by the high conversion of *o*-xylene, which is similar to the promotion effect of NO on BTEX previously reported [14]. A study showed, however, that the incorporation of sulfate ion increased the photoactivity of the catalyst [46]. The higher photocatalytic activity was due to a larger surface area and the suppression of the growth of the rutile phase. The increase in surface area and the suppression of the growth of rutile phase of the catalyst was calcinated at 723 K. In this study, the sulfate ion was found owing to the adsorption of SO_2 generated from the inlet stream. The TiO_2 filter was not calcinated after the adsorption of SO_2. The surface area and the composition of anatase and rutile phase was identical prior and after the adsorption of SO_2. Thus,

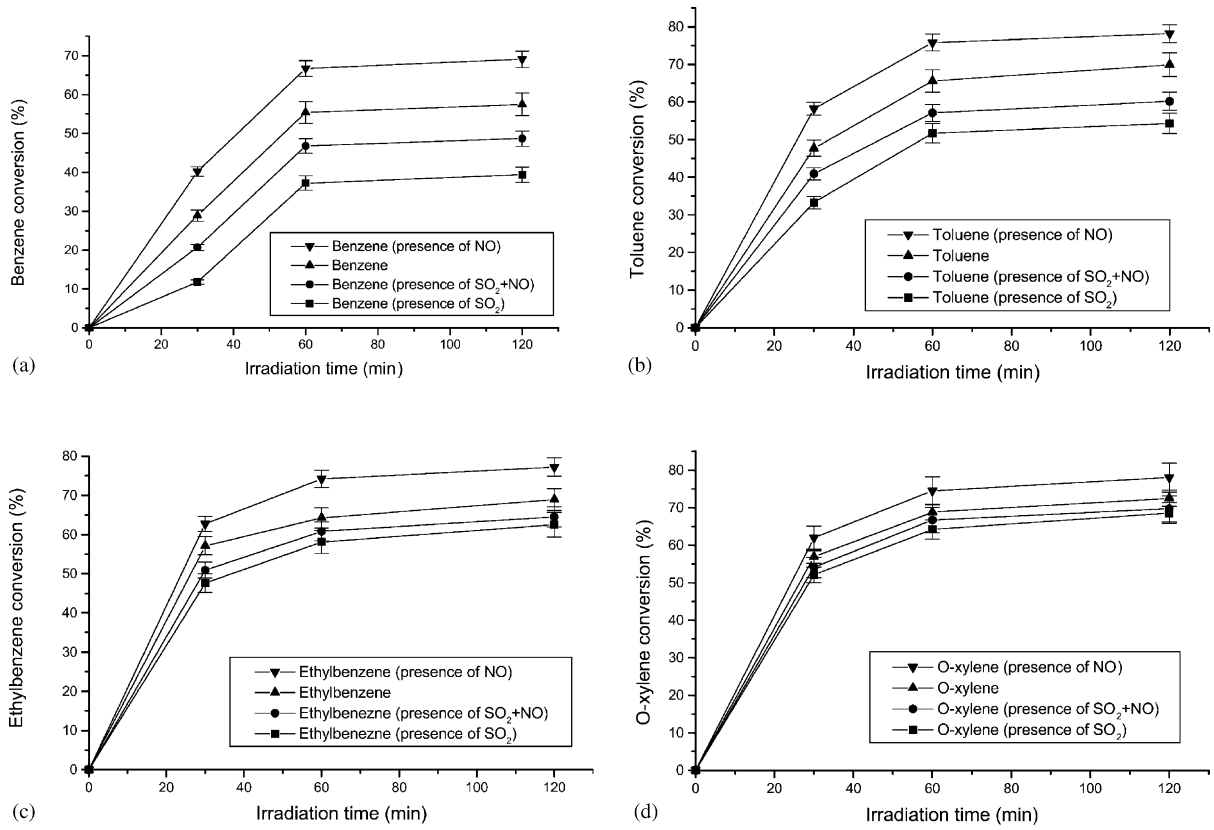

Fig. 4. (a) Benzene conversion with respect to the irradiation time. Experimental conditions—residence: 1.2 min; humidity level: 2100 ppmv. (■) Presence of 200 ppb SO_2; (●) presence of 200 ppb SO_2 and NO; (▲) presence of benzene only; (▼) presence of 200 ppb NO. (b) Toluene conversion with respect to the irradiation time. Experimental conditions—residence time: 1.2 min; humidity level: 2100 ppmv. (■) Presence of 200 ppb SO_2; (●) presence of 200 ppb SO_2 and NO; (▲) presence of benzene only; (▼) presence of 200 ppb NO. (c) Ethylbenzene conversion with respect to the irradiation time. Experimental conditions—residence time: 1.2 min; humidity level: 2100 ppmv. (■) Presence of 200 ppb SO_2; (●) presence of 200 ppb SO_2 and NO; (▲) presence of benzene only; (▼) presence of 200 ppb NO. (d) *o*-Xylene conversion with respect to the irradiation time. Experimental conditions—residence: 1.2 min; humidity level: 2100 ppmv. (■) Presence of 200 ppb SO_2; (●) presence of 200 ppb SO_2 and NO; (▲) presence of benzene only; (▼) presence of 200 ppb NO.

no increase of the photocatalytic activity was observed in this study, despite sulfate ion being found on the TiO_2 filter. Similar inhibition effect on the conversion of hydrocarbon with the presence of SO_4^{2-} ion was also reported. The inhibition effect of the sulfate ion was also observed in the photodegradation of dichloroethane (DCE). The presence of sulfate ion inhibited the adsorption and photodegradation of DCE. The major effect of the presence of sulfate ion is the competitive adsorption on the catalyst between the reactant and anion [47]. Abdullah et al. [48] also showed that the presence of sulfate ions decreased the rate of alcohol oxidation by competing adsorption sites on TiO_2 surface. The organic compounds competed with the sulfate ion for the adsorption sites on the TiO_2 surface.

Under the inhibition effect of SO_2 on BTEX and a decreased promotion effect of NO on BTEX, the conversion of BTEX with the presence of NO and SO_2 was higher than the presence of SO_2 only, but lower than BTEX only. The presence of SO_2 not only inhibited the conversion of BTEX but also inhibited the conversion of NO. According to Eq. (9), the promotion effect of NO decreased with the decreasing hydroxyl radicals formed from the photodegradation of NO. Under the inhibition effect of SO_2 on BTEX and a smaller promotion effect of NO on BTEX, the conversion of BTEX with the presence of NO and SO_2 was higher than the presence of SO_2 only, but lower than BTEX only. The highest BTEX conversion amount of the four cases was the presence of NO only. The promotion effect of NO increased the conversion of BTEX [14].

4. Conclusions

The feasibility of applying photocatalytic technology for indoor air purification using SO_2, NO, and BTEX was studied. No photodegradation of SO_2 was found under typical indoor ppb levels, but the glass fiber filter used as TiO_2 substrate adsorbed more than 75% of the SO_2. Using TiO_2 powder only without any substrate, no photodegradation or adsorption of SO_2 was observed. Sulfate ion was found after the adsorption of SO_2. The presence of SO_2 inhibited the conversion of NO and increased the generation of NO_2

by 7% and more than 10%, respectively. The formation of nitrate ion was decreased with the presence of SO_2. The inhibition effect is due to the sulfate ion competing with the pollutant for adsorption sites on TiO_2. The conversions of benzene, toluene, ethylbenzene, and *o*-xylene (BTEX) also decreased by 18, 15.6, 6.4, and 3.9%, respectively, with the presence of SO_2 compared with the photodegradation of BTEX only. The differences in the inhibition effect of SO_2 on BTEX are probably due to the reaction rate between the hydroxyl radical and BTEX being different. The promotion effect of NO on BTEX also decreases with the presence of SO_2. In essence, the conversion of BTEX with the presence of SO_2 and NO is in the following order: BTEX with SO_2 < BTEX with SO_2 and NO < BTEX < BTEX with NO. Although it is not possible to conduct simultaneous photodegradation of all the indoor air pollutants, it is inevitably valuable to investigate the effect of concurrent photodegradation of common indoor air pollutants.

Acknowledgements

This project is funded by the Hong Kong Polytechnic University (GW-047). The authors would like to thank Mr. W.F. Tam for technical support in the laboratory and Mrs. Anson for the help with the manuscript.

References

[1] A.P. Jones, Atmos. Environ. 33 (1999) 4535.
[2] L. Molhave, Indoor Air 4 (1991) 357.
[3] S.C. Lee, W.M. Li, C.H. Ao, Atmos. Environ. 36 (2002) 225.
[4] W.S. Tunnicliffe, P.S. Burge, J.G. Ayres, Lancet 344 (1994) 1733.
[5] L.A. Wallace, Environ. Health Perspect. 95 (1991) 7.
[6] M.R. Hoffmann, S.T. Martin, W. Choi, D.W. Bahnemann, Chem. Rev. 95 (1995) 69.
[7] J.C. Yu, J.G. Yu, W.K. Ho, Z.T. Jiang, L.Z. Zhang, Chem. Mater. 14 (2002) 3808.
[8] M.R. Nimlos, E.J. Wolfrum, M.L. Brewer, J.A. Fennell, G. Bintner, Environ. Sci. Technol. 30 (1996) 3102.
[9] M.A. Fox, M.T. Dulay, Chem. Rev. 93 (1993) 341.
[10] N.N. Lichtin, M. Avudaithai, E. Berman, A. Grayfer, Sol. Energy 56 (1996) 377.
[11] M.L. Sauer, M.A. Hale, D.F. Ollis, J. Photochem. Photobiol. A 88 (1995) 169.
[12] Y. Luo, D.F. Ollis, J. Catal. 163 (1996) 1.
[13] O. d'Hennezel, D.F. Ollis, J. Catal. 167 (1997) 118.
[14] C.H. Ao, S.C. Lee, C.L. Mak, L.Y. Chan, Appl. Catal. B: Environ. 42 (2003) 119.
[15] C.H. Ao, S.C. Lee, J.C. Yu, J. Photochem. Photobiol. A 156 (2003) 171.
[16] D.E. Abbey, N. Nishino, W.F. McDonnell, R.J. Burchette, S.F. Knutsen, W.L. Beeson, J.X. Yang, Am. J. Respir. Crit. Care Med. 159 (1999) 373.
[17] Environment Hong Kong, Environmental Protection Department, Hong Kong, 1997.
[18] A.J. Hedley, C.M. Wong, T.Q. Thach, S. Ma, T.H. Lam, H.R. Anderson, Lancet 360 (2002) 1646.
[19] Urban Air Pollution Control in China, China Science and Technology Press, Beijing, China, 2001.
[20] J. Shang, Y. Zhu, Y. Du, Z. Xu, J. Solid State Chem. 166 (2002) 395.
[21] C.J. Weschler, H.C. Shields, Environ. Sci. Technol. 28 (1994) 2120.
[22] C.Y. Chao, G.Y. Chan, Atmos. Environ. 35 (2001) 5895.
[23] H. Guo, S.C. Lee, W.M. Li, J.J. Cao, Atmos. Environ. 37 (2003) 73.
[24] S.C. Lee, H. Guo, W.M. Li, L.Y. Chan, Atmos. Environ. 36 (2002) 1929.
[25] L. Limousy, H. Mahzoul, J.F. Brilhac, P. Gilot, F. Garin, G. Marie, Appl. Catal. B: Environ. 42 (2003) 237.
[26] Y. Chen, J. Yi, W. Li, R. Jin, S. Tang, W. Hu, Catal. Today 50 (1999) 39.
[27] D.I. Sayago, P. Serrano, O. Bohme, A. Goldoni, G. Paolucci, E. Roman, J.A. Martin-Gago, Surf. Sci. 482–485 (2001) 9.
[28] C.H. Ao, S.C. Lee, Appl. Catal. B: Environ. 44 (2003) 191.
[29] J.H. Seinfeld, S.N. Pandis, Atmospheric Chemistry and Physics: From Air Pollution to Climate Change, Wiley, New York, 1998.
[30] A.V. Vorontsov, E.N. Savinov, E.N. Kurkin, O.D. Torbova, V.N. Parmon, React. Kinet. Catal. Lett. 62 (1997) 83.
[31] E. Meszaros, Atmospheric Chemistry: Fundamental Aspects, Elsevier, Amsterdam, 1981, p. 141.
[32] D.A. Hegg, P.V. Hobbs, Atmos. Environ. 12 (1978) 241.
[33] T.E. Graedel, Chemical Compounds in the Atmosphere, Academic Press, New York, 1978, p. 30.
[34] D. Wang, W. Deng, Water Air Soil Pollut. 130 (2001) 1631.
[35] L. Gimeno, E. Marin, T. del Teso, S. Bourhim, Sci. Total Environ. 275 (2001) 63.
[36] J.G. Henry, G.H. Heinke, Environmental Science and Engineering, Prentice-Hall, London, 1996, p. 122.
[37] R.W. Boubel, D.L. Fox, D.B. Turner, A.C. Stern, Fundamentals of Air Pollution, Academic Press, London, 1994, p. 150.
[38] K. Oilawa, K. Murano, Y. Enomoto, K. Wada, T. Inomata, J. Chromatogr. A 671 (1994) 211.
[39] K. Tanaka, K. Ohta, P.R. Haddad, J.S. Fritz, K.P. Lee, K. Hasebe, A. Ieuji, A. Miyanaga, J. Chromatogr. A 850 (1999) 311.
[40] Y. Komazaki, H. Shimizu, S. Tanaka, Atmos. Environ. 33 (1999) 4363.
[41] S. Matsuda, H. Hatano, A. Tsutsumi, Chem. Eng. J. 82 (2001) 183.
[42] K. Hashimoto, K. Wasada, M. Osaki, E. Shono, K. Adachi, N. Toukai, H. Kominami, Y. Kera, Appl. Catal. B: Environ. 30 (2001) 429.
[43] T. Ibusuki, K. Takeuchi, J. Mol. Catal. 88 (1994) 93.
[44] M. Sokmen, A. Ozkan, J. Photochem. Photobiol. A 147 (2002) 77.
[45] R. Atkinson, Atmos. Environ. A 24 (1990) 1.
[46] X. Fu, Z. Ding, W. Su, Chin. J. Catal. 20 (1999) 321.
[47] H.Y. Chen, O. Zahraa, M. Bouchy, J. Photochem. Photobiol. A 108 (1997) 37.
[48] M. Abdullah, G.K.C. Low, R.W. Matthews, J. Phys. Chem. 94 (1990) 6820.